JPPIPA 11(9) (2025)

Jurnal Penelitian Pendidikan IPA

http://jppipa.unram.ac.id/index.php/jppipa/index

Identification of Cumulonimbus Clouds as a Trigger for Extreme Weather at Soekarno-Hatta International Airport on July 24, 2023 Based on Weather Radar, LIDAR, and PWV Estimates of the ECMWF-ERA5 Numerical Model

Aliyatus Saadah[1,2*], Mokhamad Nur Cahyadi[1]

[1] Department of Geomatics Engineering, Faculty of Civil, Planning, and Earth Engineering, Sepuluh Nopember Institute of Technology, Kampus ITS Sukolilo, Surabaya, Indonesia.
[2] Badan Meteorologi, Klimatologi dan Geofisika, Indonesia.

Received: July 06, 2025
Revised: August 20, 2025
Accepted: September 25, 2025
Published: September 30, 2025

Corresponding Author:
Aliyatus Saadah
aliyatus.saadah@bmkg.go.id

DOI: 10.29303/jppipa.v11i9.12604

Abstract: Cumulonimbus (CB) clouds are a significant weather threat to flight safety and efficiency in tropical regions such as Indonesia. CB clouds are cloud that aircraft must avoid because they contain rising and falling air currents that can suck and blow aircraft away. This study aims to identify the characteristics of CB clouds that triggered extreme weather disturbances at Soekarno-Hatta International Airport on July 24, 2023. The analysis was conducted through a descriptive-integrative approach by utilizing Precipitable Water Vapor (PWV) estimation data from the ECMWF-ERA5 reanalysis numerical model, weather radar (CMAX and HSHEAR products), and Light Detection and Ranging (LIDAR). The analysis results indicate significant moisture accumulation before the event, characterized by an increase in PWV values up to 41.50–47.60 kg/m², creating atmospheric conditions that are very supportive of the formation of convective clouds. During the event, weather radar detected strong convection through high reflectivity values (> 60 dBZ) and horizontal shear exceeding 10 m/s/km. Simultaneously, LIDAR data identified the life cycle of CB clouds, from the initiation (inflow) to the decay (outflow) phase. This extreme weather event directly impacted flight operations, resulting in nine go-around reports and four diverts. These findings confirm that multi-sensor data integration can effectively enhance CB cloud early detection capabilities and strengthen weather risk mitigation systems for aviation safety at high-traffic airports.

Keywords: Aviation; Cumulonimbus; Extreme weather; LIDAR; PWV; Weather radar

Introduction

In tropical regions like Indonesia, one of the significant weather threats to flight safety and efficiency is Cumulonimbus (CB) clouds. As a major hub for national aviation activity, Soekarno-Hatta Airport, with an average of 1.200 aircraft movements per day, is characterized by the frequent formation of Cumulonimbus clouds, which can cause adverse weather conditions such as turbulence, lightning, heavy rain, and wind shear (Abbasi et al., 2021; Storer et al., 2019). One of the main threats to flight safety and efficiency is the presence of Cumulonimbus (CB) clouds, which are highly destructive and dark in color when mature (Hentzen et al., 2018). Natural events that accompany this phase include dropping air

How to Cite:
Saadah, A., & Cahyadi, M. N. (2025). Identification of Cumulonimbus Clouds as a Trigger for Extreme Weather at Soekarno-Hatta International Airport on July 24, 2023 Based on Weather Radar, LIDAR, and PWV Estimates of the ECMWF-ERA5 Numerical Model. *Jurnal Penelitian Pendidikan IPA*, *11*(9), 395–406. https://doi.org/10.29303/jppipa.v11i9.12604

temperature, strong wind gusts, heavy rain with or without thunderstorms, tornadoes, turbulence, aircraft icing, squall or gusty weather, and even hail (Somorowska, 2023; Belioka & Achilias, 2024). This study aims to analyze selected extreme weather events affecting the operational area of Soekarno-Hatta International Airport by utilizing ground-based weather radar data, Precipitable Water Vapor (PWV) data obtained from the ECMWF-ERA5 numerical model, and remote sensing from Light Detection and Ranging (LIDAR). The integration of these data sources allows for a comprehensive understanding of atmospheric water content and convective activity (Agyekum et al., 2024; Baldysz et al., 2024; Lou et al., 2021).

The extreme weather event that occurred on July 24, 2023, in the vicinity of Soekarno-Hatta Airport provides clear evidence that convective clouds, such as Cumulonimbus (CB) clouds, can significantly impact flight operations. Cumulonimbus clouds are cloud that aircraft must avoid because they contain ascending and descending air currents that can suck and blow aircraft away (Belo-Pereira, 2025; Kwasiborska et al., 2023). Atmospheric conditions during extreme weather events are characterized by increased water vapor content in the lower to middle atmosphere, as well as significant instability that supports rapid vertical cloud growth. This causes disruptions in the form of diverted landings, canceled landings (go-arounds), and flight delays due to reduced visibility and the intensity of the heavy rain (Lakra & Avishek, 2022). This case was chosen because, based on Air Navigation (AirNav) data, there were 9 cases of aircraft going around and 4 cases of diverting (Sun et al., 2024; Liu et al., 2021). This study on the identification of cumulonimbus clouds is expected to assist in providing information and early warnings to stakeholders, particularly air navigators.

On the other hand, the challenge of accurately monitoring and predicting the presence of convective clouds remains a challenge in aviation weather early warning systems (Reichstein et al., 2025; Xue et al., 2025; Lean et al., 2024). The use of multi-source observation technologies such as weather radar, LIDAR, and GNSS is crucial to improve the accuracy of early detection of convective clouds. Previous studies have shown that GNSS has good capabilities in monitoring atmospheric water vapor content through the Precipitable Water Vapor (PWV) parameter, which can be used to detect atmospheric conditions before and after extreme events such as heavy rainfall or volcanic eruptions (Cahyadi et al., 2017; Cahyadi et al., 2024). Weather radar can provide spatial and temporal information on the structure and intensity of cloud precipitation, while PWV provides an overview of the distribution of water vapor, which provides latent convective energy, while LIDAR supports the identification of the height and vertical distribution of atmospheric particles, including clouds and aerosols (He et al., 2021; Jin et al., 2024). By combining these three data sources, a more in-depth analysis of the formation and evolution mechanisms of cloud-borne convection clouds can be conducted in a more holistic manner.

Furthermore, this study also aligns with the need to improve extreme weather risk monitoring and mitigation systems in areas with high traffic international airports. Through an integrative approach based on observations and spatial-temporal analysis, this research is expected to contribute to the development of an early warning system based on advanced science and technology that is more adaptive to the characteristics of Indonesia's tropical climate.

Method

This study uses observational data from several meteorological and remote sensing instruments to identify and analyze Cumulonimbus (CB) clouds that caused extreme weather at Soekarno-Hatta Airport on July 24, 2023. The data used in this study are:

Weather Radar Data (CMAX and HSHEAR)

Weather radar data was collected from a C-band radar located in Tangerang City. The temporal resolution of the data is every 8 minutes from 03:00 UTC to 09:00 UTC, covering the periods before, immediately after, and after the extreme weather event. The radar products analyzed are:

CMAX (Composite Maximum Reflectivity)

This radar product displays the maximum reflectivity value from all radar scan elevations. This product is very useful for detecting the position and intensity of maximum precipitation or high reflectivity associated with CB clouds (Chen et al., 2022; Li et al., 2023).

HSHEAR (Horizontal Shear)

This product can detect the presence and strength of horizontal wind shear within an atmospheric layer. HSHEAR can indicate the potential for wind shear to be hazardous to aviation, especially around cloud-like clouds.

LIDAR (Light Detection and Ranging) Data

The LIDAR data used is vertical atmospheric data from 04:00 UTC to 08:00 UTC on July 24, 2023. The LIDAR instrument is used to detect the vertical distribution of atmospheric particles such as clouds, aerosols, and dew. With its high spatial and temporal resolution, LIDAR helps identify periods in the life cycle of cloud-like clouds.

ECMWF-ERA5 Numerical Model Data

The numerical model data used in this study is surface dew point temperature data obtained from https://cds.climate.copernicus.eu/datasets/reanalysis-era5-single-levels. The model data used was from 17:00 UTC (12:00 AM WIB) on July 23, 2023, to 16:00 UTC (11:00 PM WIB) on July 24, 2023, with a temporal resolution of 1 hour. The spatial grid resolution of the model data is ~31 km, and the locations analyzed in this study are:

Table 1. Research Locations

Location	Longitude (⁰E)	Latitude (⁰S)
Soetta	106.679	-6.123
CJKU	106.842	-6.155
CJKT	106.884	-6.110
CTGR	106.663	-6.290

The processing of ECMWF-ERA5 numerical model data in GRIB format is processed using Google Earth Engine and the model output is displayed in the form of graphs and contour maps created using Python. The calculation process for the PWV value is obtained from the reduction in the surface dew point temperature value using the formula used by (Yan et al., 2024) namely:

$$ln(PWV) = a + bT_d \quad (1)$$

Where T_d = dew point temperature (°C), $a = 0.1102$, and $b = 0.06141$, and PWV value in units kg/m². The a and b values are empirical constants adapted from fitting ERA5 data in the tropical region (Indonesia). After obtaining the model's PWV estimate, the PWV value from the ECMWF-ERA5 numerical model was validated using GPS sensor observation data around Soekarno-Hatta International Airport (CJKU, CJKT, and CTGR). This data was processed using Python to generate Mean Absolute Error (MAE), Root Mean Square Error (RMSE), and correlation values. Furthermore, a scatter plot was used to assess the extent of the data deviation between the model's PWV and GPS-based observations.

This study employed a descriptive-integrative analysis method. This method was used to interpret atmospheric dynamics and identify Cumulonimbus (CB) clouds that occurred on July 24, 2023, in the Soekarno-Hatta International Airport area. Data from the three observation sources were integrated spatially and temporally to understand the relationship between water vapor increase (PWV), radial wind speed movement of CB clouds (LIDAR), and convective activity detection (RADAR). CB cloud detection results and atmospheric conditions are compared with flight operational disruption data (go-arounds and diverts) to assess the impact of extreme weather on flight safety and efficiency. Using a descriptive approach, this study seeks to provide a comprehensive understanding of the atmospheric dynamics underlying Cumulonimbus cloud formation and its impact on aviation, based on real-world observational data from various meteorological instruments.

Result and Discussion

Validation and Analysis of Precipitable Water Vapor (PWV) from the ECMWF-ERA5 Numerical Model and GPS Observations

This analysis aims to identify the water vapor distribution process at the time of the event and evaluate the performance of the ECMWF-ERA5 reanalysis model in estimating Precipitable Water Vapor (PWV) values using observational data from GPS stations as ground truth. The use of GNSS for PWV estimation has been proven effective in various previous studies, including in monitoring regional weather changes, as conducted by Sudantha et al. (2021). In general, Figure 1 shows that the model's PWV values tended to decrease gradually from morning to midday (between 00:00 and 05:00 UTC), particularly at the CTGR location, which recorded a decrease of up to 41.80 kg/m², while other locations remained above 43 kg/m². This indicates relatively stable atmospheric conditions that were not yet saturated enough to form a strong convective cloud system. Starting at 06:00 UTC, a significant spike in PWV values occurred simultaneously across all locations, indicating moisture accumulation in the lower to middle layers of the atmosphere.

This increase was most pronounced during the period 06:00–08:00 UTC, where PWV values increased from approximately 43.0 to 47.0 kg/m² at Central Jakarta (CJKU); 44.50 to 46.30 kg/m² at Central Jakarta (CJKT); and 44.3 to 46.0 kg/m² at Soetta. Peak humidity was recorded between 12:00–14:00 UTC, with the highest value reaching 47.6 kg/m² at Central Jakarta (CJKU). This spike indicates that atmospheric conditions have reached a saturated phase, which strongly supports the vertical growth of convective clouds such as Cumulonimbus (CB). To support spatial diagnosis, Figure 2 displays PWV contour maps interpolated from model data at six times: 00, 03, 06, 09, 12, and 15 UTC, or 07:00, 10:00, 13:00, 16:00, 19:00, and 22:00 WIB. Analysis of the evolution of atmospheric humidity shows a pattern in the morning (00 UTC / 07:00 WIB and 03 UTC/ 10:00 WIB) where the PWV distribution value appears uniform across the study area. Values range from 43–45 kg/m², as indicated by the dominance of blue and green colors on the map.

At this stage, there is no apparent accumulation or dominance of moisture in certain areas, indicating

relatively stable atmospheric conditions. During the day (06 UTC/13:00 WIB) the PWV value shows a slight decrease and becomes more evenly distributed across the area, with values in the range of 42–43 mm. At this time, no significant increase in humidity was observed. Furthermore, from 07 UTC (14:00 WIB) to 09 UTC (16:00 WIB), the most significant change in PWV values occurred, with PWV values at almost all points increasing drastically, exceeding 46 mm (marked in yellow and orange). The highest humidity centers appeared concentrated in the northeast (around Central Jakarta and Central Jakarta), indicating a water vapor supply and the possibility of strong local convergence, which is beginning to strengthen atmospheric instability. This spatial and temporal pattern is consistent with research (Benevides et al., 2015) which states that a PWV increase of ≥2 mm or kg/m2 within <3 hours can serve as an early indicator of convective cloud formation and local rainfall.

In this case, the sharp increase in PWV between 06:00–08:00 UTC indicates the initiation phase of convection, which then develops into an active convective cloud system. Furthermore, these findings reinforce the recommendation of Suparta et al. (2016), who highlighted the importance of monitoring GPS-based PWV fluctuations as an indicator of extreme weather in tropical regions. High PWV values indicate a large release of latent energy, which initiates and sustains convective systems. These results are also consistent with studies by Zhang et al. (2019) and Santos et al. (2022) who concluded that a rapid and uniform PWV surge is one of the early signals of the formation of multi-cell cloud systems and squall lines. Compared with the results of research by Wu et al. (2022), which recorded PWV values in the Surabaya area ranging from 25.13 to 32.87 mm with an average of 27.38 mm during the transition period from the dry season to the rainy season, the PWV values in this study—which reached up to 47.60 kg/m²—indicate much more saturated and unstable atmospheric conditions. This significant difference indicates that the extreme weather event at Soekarno-Hatta International Airport on July 24, 2023, occurred in an atmospheric environment that strongly supports the formation of convective clouds such as CB clouds.

Furthermore, the results of research Hsiung et al. (2024), also show that PWV values above 40 mm in urban coastal areas such as Jakarta and its surroundings are a strong indicator of the potential for the development of intense convective activity and extreme weather events. Thus, these findings further emphasize the importance of PWV monitoring, particularly GNSS-based monitoring, as a key parameter in the early detection and forecasting of extreme weather, both in the context of seasonal changes and extreme weather events, as examined in this study. Figure 3 shows a graphical comparison of PWV values from the ECMWF-ERA5 model and GPS sensor observations. Because there are no PWV observation data at the Soetta point, the Soetta point could not be validated and was not included in this validation analysis. The validation analysis results show that the model line (in blue) tends to be smoother than the observation line (in orange), indicating sharper variability and higher frequency. This occurs due to a common phenomenon in numerical models. The ERA5 model, with a spatial resolution of ~31 km, represents the average value within a single grid cell, thus tending to "average" the extreme peaks and valleys captured by point instruments such as GPS.

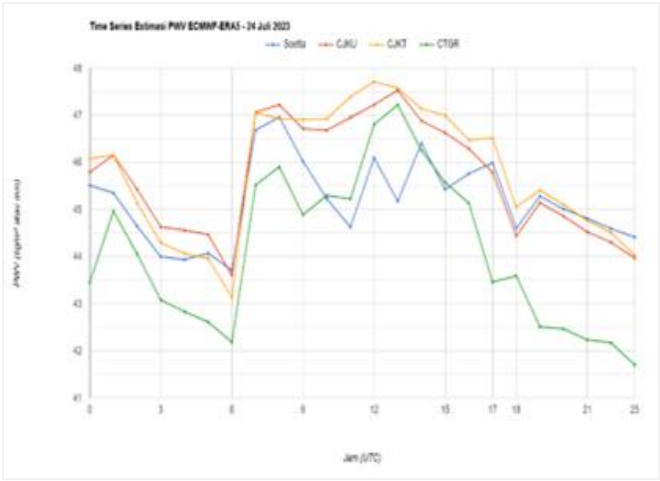

Figure 1. Time series graph of PWV Estimates from the ECMWF-ERA5 model

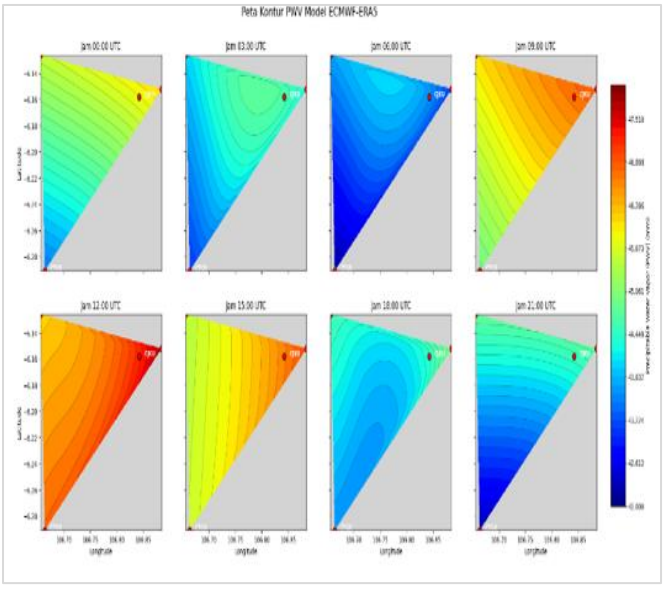

Figure 2. Contour map of PWV estimates from the ECMWF-ERA5 model

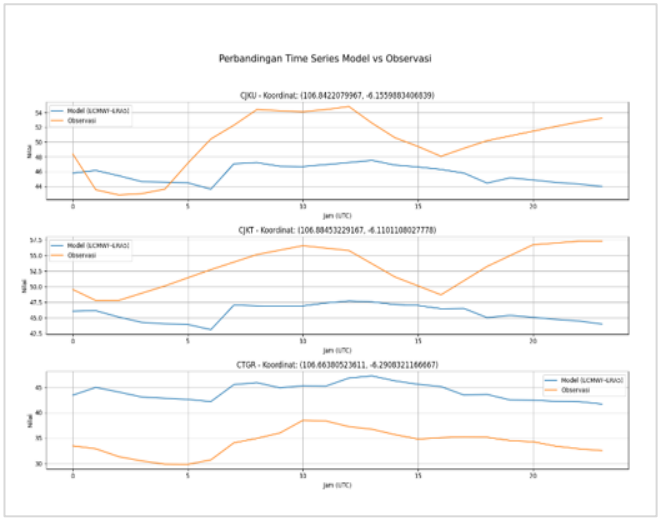

Figure 3. Comparison of validation results of precipitable water vapor (PWV) values from the ECMWF-ERA5 model and GPS sensors

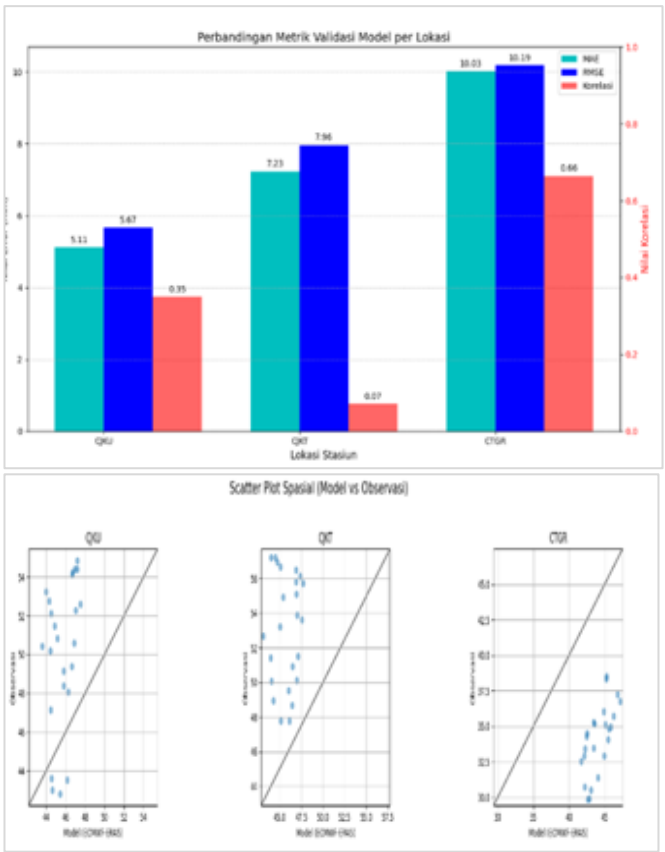

Figure 4. Comparison chart of model validation metrics per GPS sensor location and spatial scatterplot to assess the accuracy of the PWV model from ECMWF-ERA5 with GPS sensors

Although, according to Hersbach et al. (2020), the ERA5 model is recognized as a significant improvement over ERA-Interim, like other models, ERA5 is not perfect and does exhibit some limitations, particularly its inability to accurately represent the amplitude of the diurnal PWV cycle. The observational data (orange line) in Figure 3 shows strong diurnal fluctuations, which may not be fully captured by the model. The model may exhibit bias, either due to a slight time lag or by underestimating the difference between the maximum (daytime) and minimum (early morning) PWV values. Figure 4 shows a graph of model validation metrics per location and a spatial scatterplot to assess the accuracy of the ECMWF-ERA5 model PWV (x-axis) and GPS observations (y-axis). The correlation value indicates the degree of linear relationship between the model and observations. Station CTGR shows the highest correlation (0.66), indicating a moderate positive relationship. In contrast, station CJKT has a very low correlation (0.07), indicating that the ERA5 model struggles to track PWV variations at this location. CJKU is in between with a correlation of 0.35. This difference in values between locations demonstrates the importance of locally validating PWV values, as model accuracy is not spatially uniform.

RMSE measures the standard deviation of the difference (error) between the model and observations, and provides an overview of the average error magnitude in mm. RMSE values at the three locations ranged from 5.67 mm to 10.19 mm. This value is consistent with the results of ECMWF-ERA5 validation studies in other regions. For example, Guo et al. (2024) found RMSE ranging from 2-4 mm in China, and Majidi et al. (2025), validated a numerical model with RMSE values of around 3-5 mm in Portugal. The slightly higher RMSE value in the Jakarta region can be attributed to the complexity of the tropical atmosphere, which has a higher water vapor content and is more dynamic. The distribution of points in the scatter plot provides a visual illustration of model bias. For CTGR, the points tend to cluster around the 1:1 line, albeit with a fairly wide spread. For CJKU and especially CJKT, the points are very spread out and far from the 1:1 line, confirming a low correlation. An indication of model bias is seen in that when the observed PWV value is high (with a value > 50 mm), the points tend to be below the 1:1 line. This indicates that the ECMWF-ERA5 model has a tendency to underestimate the PWV value of GPS observations when atmospheric conditions are very humid.

Spatial Evolution of Cumulonimbus Cloud Growth Based on Weather Radar Data

The CMAX radar product represents the maximum radar reflectivity value within the entire vertical scan volume. This product is widely used to identify strong convective clouds, such as Cumulonimbus (CB), which are characterized by high reflectivity and deep vertical structure (Harasti et al., 2015). Reflectivity values ≥45 dBZ are typically associated with heavy precipitation, turbulence, or even the possibility of hail (Müller et al.,

2018). In the July 24, 2023, CMAX radar analysis from 03:55 UTC to 08:35 UTC showed significant convective cloud development that directly impacted the operational area of Soekarno-Hatta Airport. Figure 5 shows the spatial evolution and reflectivity intensity of CB clouds from 03:55 UTC to 08:51 UTC. Several convective cloud cells with reflectivities of 45–50 dBZ were observed in the Tangerang, West Jakarta, and East Jakarta areas. The cloud cells appeared to be beginning to develop vertically and exhibited a locally active multi-cell structure. This stage indicates the initial convection process in an unstable atmospheric environment, supported by adequate humidity, as shown in Figure 1.

Cloud growth occurred southwest of Soekarno-Hatta Airport at 03:55 UTC (10:55 WIB), with a maximum reflectivity value reaching 39 dBZ. The clouds remained localized, but some cells showed significant potential for vertical growth. The cloud development continued and moved north and eastward until entering Soekarno-Hatta Airport at 05:15 UTC (12:15 WIB), with a maximum reflectivity value reaching 51 dBZ. After the cloud entered Soekarno-Hatta Airport, the cloud continued to grow above the airport until it reached the highest maximum reflectivity value of >60 dBZ at 05.39 UTC or 12.39 WIB. According to Mandú et al. (2024), reflectivity values ≥55 dBZ at the upper atmospheric level (5–8 km) are often associated with mature cloud structures. This activity coincided with operational reports of several go-arounds and diverts, confirming the potential for significant disruption to flight safety. Several aircraft reportedly experienced go-arounds and diverts, as shown in Table 2.

At 06:19 UTC (13:19 WIB), the cloud system became increasingly elongated and merged, forming a quasi-linear convective system, as described in Zheng et al. (2022), stretching from south to north past Soekarno-Hatta Airport. Reflectivity values >65 dBZ were observed at several points, indicating very strong precipitation and the potential for lightning/gust fronts, as described in (Lang, 2020). Convective activity at this time marked the peak of the extreme weather event. The clouds then began to dissipate at 08:03 UTC (3:03 PM WIB) and continued until 08:51 UTC (3:51 PM WIB), marked by a gradual shift of clouds northward and a weakening of maximum cloud reflectivity values. The CMAX product proved to be an effective early indicator for detecting and monitoring active CB clouds spatially and temporally. In this case, high reflectivity was consistently detected over the airport area. When integrated with PWV and LIDAR data, the use of CMAX radar becomes a crucial component of an early warning system for aviation safety, as suggested in recent studies (Konopka & Rzucidło, 2025).

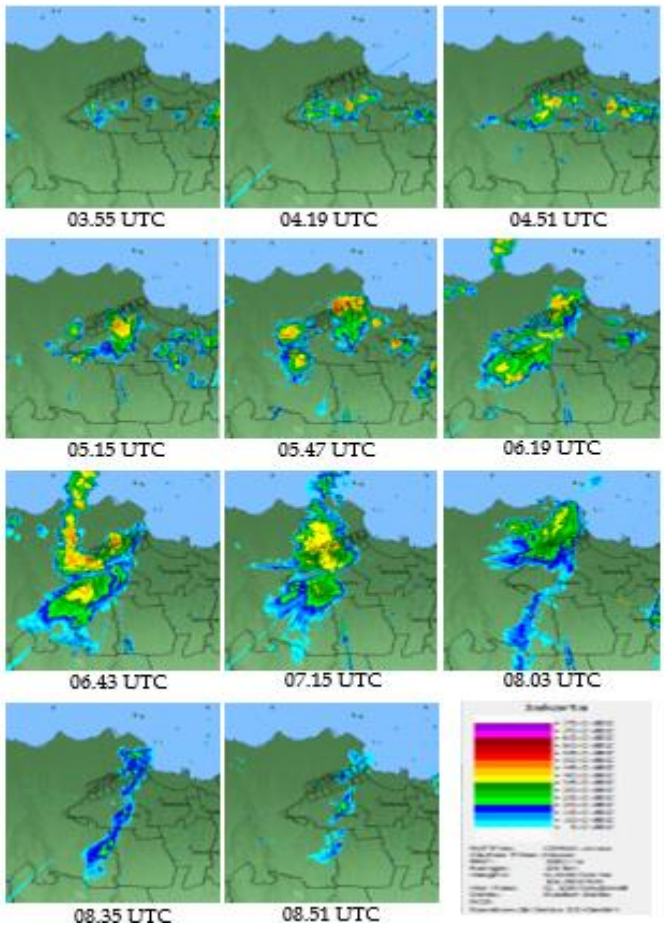

Figure 5. CMAX radar product showing

Table 2. Flight data impacted by CB clouds obtained from AirNav in 2023

Time (UTC)	Category	Flight ID	Operator	Airport of Origin	Reason	Pilot Report Contents
05:15	sGO AROUND	GIA291	GARUDA INDONESIA	WARA	weather	AT 0515 UTC GIA291/PKGFG/B738/WARA-WIII GO ROUND RWY 25L DUE TO TAIL WIND. LANDED RWY 25L AT 05.33 UTC
05:17	Divert	CTV763	CITILINK	WAHQ	weather	AT 0517 UTC CTV763/A320/PKGLW/WAHQ-WIII, GO ROUND RWY 25L DUE TO UNSTABLE APPROACH THEN DIVERT TO WAHS DUE TO WEATHER.

Time (UTC)	Category	Flight ID	Operator	Airport of Origin	Reason	Pilot Report Contents
05:17	GO AROUND	CTV763	CITILINK	WAHQ	unstable approach	AT 0517 UTC CTV763/A320/PKGLW/WAHQ-WIII, GO ROUND RWY 25L DUE TO UNSTABLE APPROACH THEN DIVERT TO WAHS DUE TO WEATHER.
05:22	GO AROUND	LNI809	LION AIR	WIJJ	windshear	AT 0522 UTC LNI809/PKLQT/B739/WIJJ-WIII, GO ROUND RWY 25R DUE TO TAIL WIND AND WIND SHEAR, REPORT SHORT OF FUEL. LANDED RWY 07R AT 0553 UTC
05:37	Divert	CSN3037	CHINA SOUTHERN	ZGGG	windshear	AT 0537 UTC CSN3037/B3206/A21N/ZGGG-WIII GO AROUND RWY 25L DUE TOWIND SHEAR THEN DIVERT TO WAHS.
05:37	GO AROUND	CSN3037	CHINA SOUTHERN	ZGGG	windshear	AT 0537 UTC CSN3037/B3206/A21N/ZGGG-WIII GO AROUND RWY 25L DUE TOWIND SHEAR THEN DIVERT TO WAHS.
06:14	GO AROUND	GIA873	GARUDA INDONESIA	VHHH	windshear	AT 0614 UTC GIA873/PKGPU/A333/VHHH-WIIII GO AROUND RWY 07L DUE TOWIND SHEAR. LANDED RWY 07R AT 0640 UTC.
06:22	Divert	GIA327	GARUDA INDONESIA	WARR	weather	AT 0622 UTC GIA 327/B738/PKGMV, WARR-WIII DIVERT TO WILL DUE TO BAD WHEATHER
06:39	GO AROUND	ALK364	SRILANKAN AIRLINES	VCBI	unstable approach	AT 0639 UTC ALK364/ARANC/A21N/VCBI-WIII GO ROUND RWY 07L DUE TO UNSTABLE APPROACH, LANDED RWY 07R AT 0700 UTC.
07:00	GO AROUND	AWQ7521	INDONESIA AIR ASIA	WADD	visibility below minima	AT 0700 UTC AWQ7521/A320/PKAZJ/WADD-WIII GO AROUND RWY 07L DUE TO VISIBILITY BELOW MINIMA. LANDED RWY 25L AT 0732 UTC.
07:14	GO AROUND	SJV835	SUPER AIR JET	WIGG	visibility below minima	AT 0714 UTC SJV835/A320/PKSJK/WIGG-WIII GO AROUND RWY 07R DUE TO VISIBILITY BELOW MINIMA. LANDED RWY 25L AT 0727 UTC.
07:11	GO AROUND	BTK6183	BATIK AIR	WAAA	visibility below minima	AT 0711 UTC BTK6183/B738/PKLDO/WAAA-WIII GO AROUND RWY 07L DUE TO VISIBILITY BELOW MINIMA. AT 0730 UTC BTK6183 DIVERT TO WIPP.
07:11	Divert	BTK6183	BATIK AIR	WAAA	visibility below minima	AT 0711 UTC BTK6183/B738/PKLDO/WAAA-WIII GO AROUND RWY 07L DUE TO VISIBILITY BELOW MINIMA. AT 0730 UTC BTK6183 DIVERT TO WIPP.

Horizontal Wind Shear Dynamics Analysis

Horizontal shear (HSHEAR) data obtained from weather radar observations on July 24, 2023, shows the spatial and temporal development of wind shear in the Jakarta area and its surroundings, beginning at 04:19–08:59 UTC (Figure 6). At 04:19–04:51 UTC, shear activity

began to be detected in the southwest region of Jakarta. Horizontal shear values ranged from 1.0–5.0 m/s/km, indicating a change in wind speed that could trigger initial convection. At this stage, the impact zone was still localized. Then, at 05:23–05:55 UTC, there was a significant increase in shear intensity and distribution. Shear values reached >7.5 m/s/km, particularly around Soekarno-Hatta Airport and the northern coast of Tangerang. This high-intensity shear zone indicates the potential for strong convective cloud formation, with the possibility of developing into heavy rain or local thunderstorms. The shear pattern shows massive spatial expansion, encompassing Tangerang, West Jakarta, and parts of North Jakarta between 06:27 and 06:59 UTC. The shear distribution is widespread and exhibits an elongated pattern from southwest to northeast.

This pattern resembles the characteristics of a mesoscale convective system (MCS). According to (Takemi & Yamasaki, 2020), this configuration is often associated with increased low-layer shear and high humidity in the tropical atmosphere. Shear velocities reached 10.0 m/s/km, indicating high vertical atmospheric instability and the potential for significant turbulence, particularly for aviation. From 07:23 to 08:03 UTC, the high-shear zone remained active, indicating the weather system's movement northeastward. Shear with an intensity >7 m/s/km indicates the presence of cumulonimbus clouds and the risk of extreme weather. The maximum shear zone was still intensively detected along the west coast to North Jakarta. The shear spread toward the northeast, indicating the movement of an active weather system. Although the main concentration remained in the coastal area, the shear began to shift spatially outside radar coverage.Then, between 08:43 and 08:59 UTC, shear activity began to weaken and shrink both in intensity and impact area. The remaining shear zone was located in Tangerang and southern Jakarta, with lower shear intensity (<3 m/s/km), indicating the weakening of the convective system and its movement out of the radar observation area.

The analysis results show that the horizontal wind shear pattern is closely related to intense convective activity in and around Soekarno-Hatta Airport. A significant increase in shear during the afternoon and evening strengthens the indication of the formation of cumulonimbus clouds and a local storm system. The horizontal shear pattern observed during the observation period indicates a close relationship with convective activity in and around Jakarta, particularly Soekarno-Hatta Airport. Increased shear contributes to the formation of local thunderstorms and intense rainfall. This condition is driven by several local factors, including surface wind convergence, which is common in coastal areas, and the influence of urban heat islands, which strengthen convection processes. The influence of this horizontal shear can impact atmospheric stability and increase the potential for air turbulence around airports.

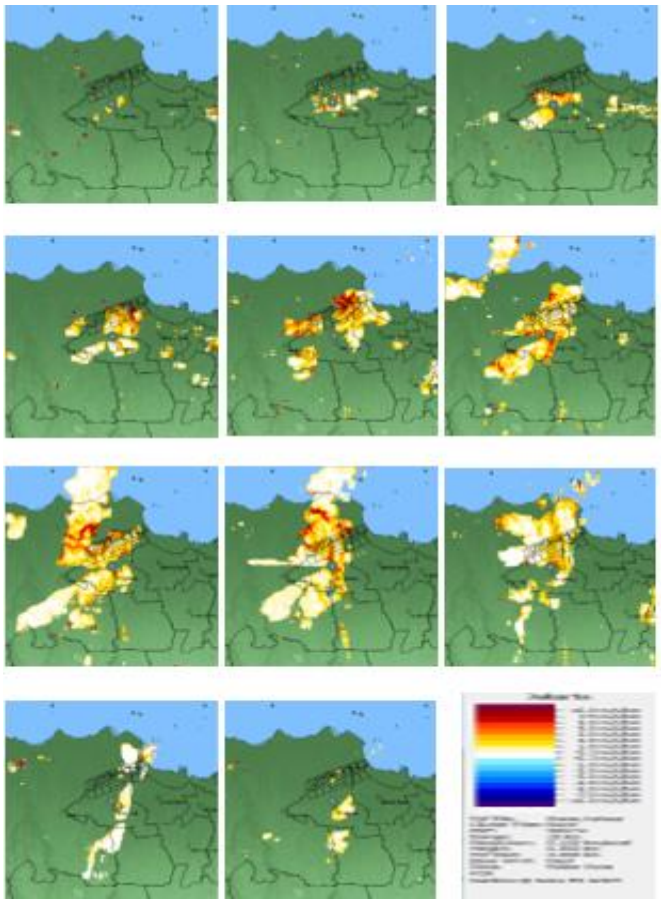

Figure 6. Weather radar SHEAR product for detecting horizontal shear generated from CB clouds

LIDAR Data Analysis

LIDAR observations were conducted between 03:55 UTC and 05:23 UTC, with radial wind speed observed within a 14-km radius from the LIDAR point. The following analysis shows radial wind dynamics indicating convective activity and the potential for Cumulonimbus (CB) cloud formation around Soekarno-Hatta Airport. Figure 4 shows the initial period (convection initiation) of cloud formation from 03:55 to 05:23 UTC. At 03:55 UTC, LIDAR detected inflow from the southwest (210°–270°) at speeds of –4 to –6 m/s, along with wind divergence. These phenomena indicate the initiation of a convective system. At 04:19 UTC, inflow from the 90°–150° sector strengthened, particularly within a 2–6 km radius. The peak occurred at 04:51 UTC, when the inflow reached –8 m/s, and the color gradient indicated an updraft within a 10-km radius of the sensor. At 05:23 UTC, the inflow weakened, and the dominance of orange in the lower layers indicated the onset of subsidence. These results align with a study by Voigt et al. (2022), which found that

LIDAR is effective in detecting atmospheric boundary dynamics and early convection processes through low-elevation, high-resolution observations.

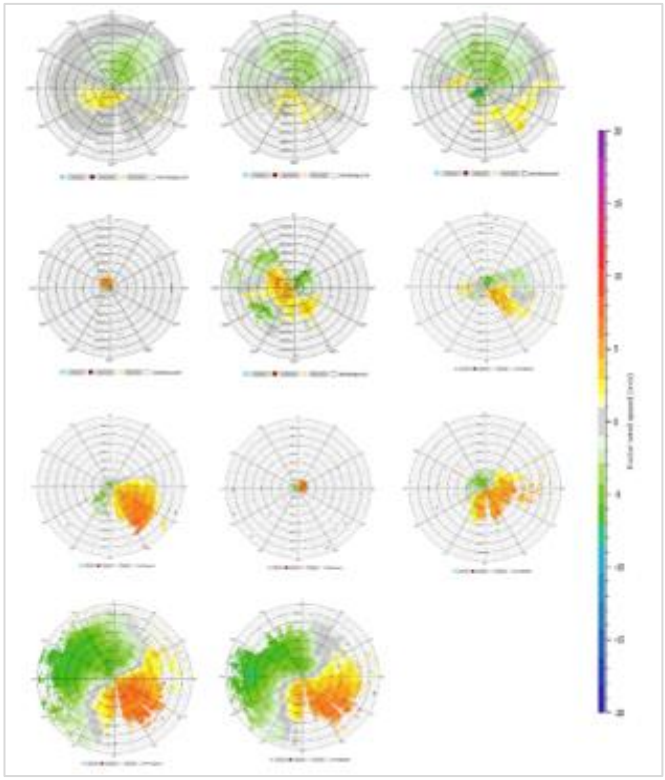

Figure 7. LIDAR image of radial wind speed (m/s) product before, immediately after, and after extreme weather events

The next period, the cloud growth period (5:55-6:27 UTC), compared with previous weather radar data (in Figure 2), shows an inflow pattern from the southeast and northwest at speeds of –4 to –8 m/s, consistent with the weakening inflow from the previous LIDAR image. This represents a transition phase from initial growth to active convection. Horizontal convergence is clearly visible, supporting the growth of convective clouds. Next, from 6:27-6:59 UTC, maximum growth occurs, with the inflow pattern strengthening from the southeast, reaching speeds of –10 m/s. This can also be detected from the radar image pattern, which shows a divergence zone in the upper layers, indicating the presence of a strong updraft and the release of latent energy (marking the peak phase of the convective cloud system). Then, from 6:59-8:03 UTC, cloud decay occurs, characterized by weakening inflow. Meanwhile, outflow begins to dominate. The horizontal spread of winds indicates that the system is beginning to lose its vertical intensity. No significant vertical cloud growth zones were detected. The convective/CB cloud system began to decay between 08:03 and 08:59 UTC, with the outlow expanding horizontally and vertically. The inflow disappeared, and the system became uniform without any convergence. This indicates the end of the CB cloud phase.

Conclusion

This study successfully identified and analyzed the dynamics of the convective system developing in the Soekarno-Hatta International Airport area on July 24, 2023, through an integrative approach using LIDAR data on radial wind speed outputs, CMAX and HSHEAR weather radar reflectivity, and calculated Precipitable Water Vapor (PWV) values from the ECMWF-ERA5 numerical model. The results indicate that the model's PWV estimates indicate a significant distribution of water vapor accumulation before and during the growth phase of the convective cloud system. High water vapor levels act as the primary latent energy supporting the convection process, as evidenced by the very high PWV values occurring concurrently with the CB cloud intensification period. The CMAX and HSHEAR radar products confirmed the presence and intensity of the convective system, with relatively high reflectivity values (>60 dBZ) and maximum horizontal shear values reaching 10 m/s/km, which consistently correlated with the period of maximum convective activity as detected by LIDAR. The LIDAR data provides an accurate representation of the distribution of inflow and outflow resulting from CB clouds, and the observed spatial and temporal variability of radial wind speeds comprehensively indicates the stages of the Cumulonimbus cloud life cycle.

Acknowledgements

The lead author expresses his deepest appreciation to the Meteorology, Climatology, and Geophysics Agency (BMKG) for its institutional support throughout this research. Special appreciation also goes to Mokhamad Nur Cahyadi from the Sepuluh Nopember Institute of Technology (ITS) Surabaya and Aries Kristianto from the College of Meteorology, Climatology and Geophysics (STMKG) for their valuable contributions in the form of advice, academic guidance, and technical assistance in the preparation of this manuscript.

Author Contributions

Conceptualization, A.S. and M.N.C.; methodology, A.S.; software, A.S.; validation, A.S. and M.N.C.; formal analysis, A.S.; investigation, A.S.; resources, A.S.; data curation, A.S.; writing—original draft, A.S.; Writing—review and editing, M.N.C.; visualization, A.S.; supervision, M.N.C.; project administration, A.S.; funding acquisition, A.S. All authors have read and approved the final version of the published manuscript.

Funding

This research was funded by the Center for Human Resource Development of the Meteorology, Climatology, and Geophysics Agency (PPSDM BMKG) through an internal

research funding scheme. Publication costs, including the Article Processing Charge (APC), were also fully covered by PPSDM BMKG.

Conflict of Interest

The authors declare that they have no conflicts of interest related to this research. Any personal or financial circumstances that could potentially influence the results have been transparently disclosed. The funding agency had no involvement in the study design, data collection, analysis, interpretation, writing of the manuscript, or the decision to publish the results.

References

Abbasi, E., Etemadi, H., Smoak, J. M., Rousta, I., Olafsson, H., Baranowski, P., & Krzyszczak, J. (2021). Investigation of Atmospheric Conditions Associated with a Storm Surge in the South-West of Iran. *Atmosphere*, *12*(11), 1429. https://doi.org/10.3390/atmos12111429

Agyekum, E. B., Odoi-Yorke, F., Mbasso, W. F., Darko, R. O., Adegboye, O. R., & Abbey, A. A. (2024). Towards a comprehensive understanding of atmospheric water harvesting technologies – a systematic and bibliometric review. *Energy Reports*, *12*, 3795–3811. https://doi.org/10.1016/j.egyr.2024.09.059

Baldysz, Z., Nykiel, G., Baranowski, D. B., Latos, B., & Figurski, M. (2024). Diurnal variability of atmospheric water vapour, precipitation and cloud top temperature across the global tropics derived from satellite observations and GNSS technique. *Climate Dynamics*, *62*(3), 1965–1982. https://doi.org/10.1007/s00382-023-07005-0

Belioka, M.-P., & Achilias, D. S. (2024). The Effect of Weathering Conditions in Combination with Natural Phenomena/Disasters on Microplastics' Transport from Aquatic Environments to Agricultural Soils. *Microplastics*, *3*(3), 518–538. https://doi.org/10.3390/microplastics3030033

Belo-Pereira, M. (2025). Forecasting Cumulonimbus Clouds: Evaluation of New Operational Convective Index Using Lightning and Precipitation Data. *Remote Sensing*, *17*(9), 1627. https://doi.org/10.3390/rs17091627

Benevides, P., Catalao, J., & Miranda, P. M. A. (2015). On the inclusion of GPS precipitable water vapour in the nowcasting of rainfall. *Natural Hazards and Earth System Sciences*, *15*(12), 2605–2616. https://doi.org/10.5194/nhess-15-2605-2015

Cahyadi, M. N., Audah, S., Mutia, N., & Aliyan, S. A. (2017). Analysis of weather changes in the region of Surabaya in 2015 and 2016 using water vapor data from GPS and Terra MODIS satellite image. In *AIP Conference Proceedings* (Vol. 1857, No. 1, p. 080003). AIP Publishing LLC. https://doi.org/10.1063/1.4987097

Cahyadi, M. N., Bawasir, A., Arief, S., Widodo, A., Rusli, M., Kusumawardani, D., Rahmawati, Y., Martina, A., Maulida, P., & Lestiana, H. (2024). Analysis of the effect of the 2021 Semeru eruption on water vapor content and atmospheric particles using GNSS and remote sensing. *Geodesy and Geodynamics*, *15*(1), 33–41. https://doi.org/10.1016/j.geog.2023.04.005

Chen, Y., Huo, J., Li, X., Bi, K., Ma, N., Jing, Y., & Ma, X. (2022). Classification and characteristic analysis of the clouds and dust in a dust-carrying precipitation process based on multi-source remote sensing observations. *Atmospheric Pollution Research*, *13*(1), 101267. https://doi.org/10.1016/j.apr.2021.101267

Guo, C., Ning, N., Guo, H., Tian, Y., Bao, A., & De Maeyer, P. (2024). Does ERA5-Land Effectively Capture Extreme Precipitation in the Yellow River Basin? *Atmosphere*, *15*(10), 1254. https://doi.org/10.3390/atmos15101254

He, Y., Xu, X., Gu, Z., Chen, X., Li, Y., & Fan, S. (2021). Vertical distribution characteristics of aerosol particles over the Guanzhong Plain. *Atmospheric Environment*, *255*, 118444. https://doi.org/10.1016/j.atmosenv.2021.118444

Hentzen, D., Kamgarpour, M., Soler, M., & González-Arribas, D. (2018). On maximizing safety in stochastic aircraft trajectory planning with uncertain thunderstorm development. *Aerospace Science and Technology*, *79*, 543–553. https://doi.org/10.1016/j.ast.2018.06.006

Hersbach, H., Bell, B., Berrisford, P., Hirahara, S., Horányi, A., Muñoz-Sabater, J., Nicolas, J., Peubey, C., Radu, R., Schepers, D., Simmons, A., Soci, C., Abdalla, S., Abellan, X., Balsamo, G., Bechtold, P., Biavati, G., Bidlot, J., Bonavita, M., … Thépaut, J. (2020). The ERA5 global reanalysis. *Quarterly Journal of the Royal Meteorological Society*, *146*(730), 1999–2049. https://doi.org/10.1002/qj.3803

Hsiung, A. R., Hartanto, R. S., Bhatia, N., & Morris, R. L. (2024). Challenges and opportunities for implementing nature-based coastal protection in an urbanised coastal city based on public perceptions. *Journal of Environmental Management*, *370*, 122620. https://doi.org/10.1016/j.jenvman.2024.122620

Jin, X., Cheng, S., Zheng, X., Ma, J., Luo, Z., Fan, G., Xiang, Y., & Zhang, T. (2024). Characteristics of Cloud and Aerosol Derived from Lidar Observations during Winter in Lhasa, Tibetan Plateau. *Remote Sensing*, *16*(12), 2074. https://doi.org/10.3390/rs16122074

Konopka, P., & Rzucidło, P. (2025). The Concept of an Early Warning System for Supporting Air Traffic Control. *Aerospace*, *12*(4), 288. https://doi.org/10.3390/aerospace12040288

Kwasiborska, A., Grabowski, M., Sedláčková, A. N., & Novák, A. (2023). The Influence of Visibility on the Opportunity to Perform Flight Operations with Various Categories of the Instrument Landing System. *Sensors*, *23*(18), 7953. https://doi.org/10.3390/s23187953

Lakra, K., & Avishek, K. (2022). A review on factors influencing fog formation, classification, forecasting, detection and impacts. *Rendiconti Lincei. Scienze Fisiche e Naturali*, *33*(2), 319–353. https://doi.org/10.1007/s12210-022-01060-1

Lang, T. J. (2020). Comparing Winds near Tropical Oceanic Precipitation Systems with and without Lightning. *Remote Sensing*, *12*(23), 3968. https://doi.org/10.3390/rs12233968

Lean, H. W., Theeuwes, N. E., Baldauf, M., Barkmeijer, J., Bessardon, G., Blunn, L., Bojarova, J., Boutle, I. A., Clark, P. A., Demuzere, M., Dueben, P., Frogner, I., De Haan, S., Harrison, D., Heerwaarden, C. V., Honnert, R., Lock, A., Marsigli, C., Masson, V., … Yang, X. (2024). The hectometric modelling challenge: Gaps in the current state of the art and ways forward towards the implementation of 100-m scale weather and climate models. *Quarterly Journal of the Royal Meteorological Society*, *150*(765), 4671–4708. https://doi.org/10.1002/qj.4858

Li, M., Cao, X., Zhang, Z., Ji, H., Zhang, M., Guo, Y., Tian, P., & Liang, J. (2023). Optical Properties and Vertical Distribution of Aerosols Using Polarization Lidar and Sun Photometer over Lanzhou Suburb in Northwest China. *Remote Sensing*, *15*(20), 4927. https://doi.org/10.3390/rs15204927

Liu, Y., Hansen, M., Ball, M. O., & Lovell, D. J. (2021). Causal analysis of flight en route inefficiency. *Transportation Research Part B: Methodological*, *151*, 91–115. https://doi.org/10.1016/j.trb.2021.07.003

Lou, H., Zhang, J., Yang, S., Cai, M., Ren, X., Luo, Y., & Li, C. (2021). Exploring the Relationships of Atmospheric Water Vapor Contents and Different Land Surfaces in a Complex Terrain Area by Using Doppler Radar. *Atmosphere*, *12*(5), 528. https://doi.org/10.3390/atmos12050528

Majidi, F., Sabetghadam, S., Gharaylou, M., & Rezaian, R. (2025). Evaluation of the performance of ERA5, ERA5-Land and MERRA-2 reanalysis to estimate snow depth over a mountainous semi-arid region in Iran. *Journal of Hydrology: Regional Studies*, *58*, 102246. https://doi.org/10.1016/j.ejrh.2025.102246

Mandú, T. B., Alves, L. E. R., Vendrasco, É. P., & Biscaro, T. S. (2024). Development of Vertical Radar Reflectivity Profiles Based on Lightning Density Using the Geostationary Lightning Mapper Dataset in the Subtropical Region of Brazil. *Remote Sensing*, *16*(20), 3767. https://doi.org/10.3390/rs16203767

Müller, R., Haussler, S., & Jerg, M. (2018). The Role of NWP Filter for the Satellite Based Detection of Cumulonimbus Clouds. *Remote Sensing*, *10*(3), 386. https://doi.org/10.3390/rs10030386

Reichstein, M., Benson, V., Blunk, J., Camps-Valls, G., Creutzig, F., Fearnley, C. J., Han, B., Kornhuber, K., Rahaman, N., Schölkopf, B., Tárraga, J. M., Vinuesa, R., Dall, K., Denzler, J., Frank, D., Martini, G., Nganga, N., Maddix, D. C., & Weldemariam, K. (2025). Early warning of complex climate risk with integrated artificial intelligence. *Nature Communications*, *16*(1), 2564. https://doi.org/10.1038/s41467-025-57640-w

Santos, J. A., & Belo-Pereira, M. (2022). Sub-Hourly Precipitation Extremes in Mainland Portugal and Their Driving Mechanisms. *Climate*, *10*(2), 28. https://doi.org/10.3390/cli10020028

Somorowska, U. (2023). Warming Air Temperature Impacts Snowfall Patterns and Increases Cold-Season Baseflow in the Liwiec River Basin (Poland) of the Central European Lowland. *Resources*, *12*(2), 18. https://doi.org/10.3390/resources12020018

Storer, L. N., Williams, P. D., & Gill, P. G. (2019). Aviation Turbulence: Dynamics, Forecasting, and Response to Climate Change. *Pure and Applied Geophysics*, *176*(5), 2081–2095. https://doi.org/10.1007/s00024-018-1822-0

Sudantha, I. M., & Suwardji, S. (2021). The effect of biocompost Trichoderma spp. Tablet in stimulating shallot growth and yield for climate change adaptation. *IOP Conference Series: Earth and Environmental Science*, *824*(1), 012033. https://doi.org/10.1088/1755-1315/824/1/012033

Sun, X., Zheng, C., Wandelt, S., & Zhang, A. (2024). Airline competition: A comprehensive review of recent research. *Journal of the Air Transport Research Society*, *2*, 100013. https://doi.org/10.1016/j.jatrs.2024.100013

Suparta, W., & Alhasa, K. M. (2016). Modeling of Precipitable Water Vapor Using an Adaptive Neuro-Fuzzy Inference System in the Absence of the GPS Network. *Journal of Applied Meteorology and Climatology*, *55*(10), 2283–2300. https://doi.org/10.1175/JAMC-D-15-0161.1

Takemi, T., & Yamasaki, S. (2020). Sensitivity of the Intensity and Structure of Tropical Cyclones to Tropospheric Stability Conditions. *Atmosphere*,

11(4), 411. https://doi.org/10.3390/atmos11040411

Voigt, C., Lelieveld, J., Schlager, H., Schneider, J., Curtius, J., Meerkötter, R., Sauer, D., Bugliaro, L., Bohn, B., Crowley, J. N., Erbertseder, T., Groß, S., Hahn, V., Li, Q., Mertens, M., Pöhlker, M. L., Pozzer, A., Schumann, U., Tomsche, L., … Rapp, M. (2022). Cleaner Skies during the COVID-19 Lockdown. *Bulletin of the American Meteorological Society*, *103*(8), E1796–E1827. https://doi.org/10.1175/BAMS-D-21-0012.1

Wu, B., Wei, M., Li, Y., Wang, Z., Du, S., & Zhao, C. (2022). Analysis of the Characteristics and Evolution Mechanisms of a Bow-Shaped Squall Line in East China Observed with Dual-Polarization Doppler Radars. *Remote Sensing*, *14*(15), 3531. https://doi.org/10.3390/rs14153531

Xue, J., Yuan, C., Qu, Y., & Huang, Y. (2025). Observation of Multilayer Clouds and Their Climate Effects: A Review. *Atmosphere*, *16*(6), 692. https://doi.org/10.3390/atmos16060692

Yan, X., Yang, W., Ding, N., Gao, F., & Peng, Y. (2024). Improving MODIS-IR precipitable water vapor based on the FIDWFT model. *Advances in Space Research*, *73*(10), 4903–4921. https://doi.org/10.1016/j.asr.2024.02.036

Zhang, Y., Liu, L., Bi, S., Wu, Z., Shen, P., Ao, Z., Chen, C., & Zhang, Y. (2019). Analysis of Dual-Polarimetric Radar Variables and Quantitative Precipitation Estimators for Landfall Typhoons and Squall Lines Based on Disdrometer Data in Southern China. *Atmosphere*, *10*(1), 30. https://doi.org/10.3390/atmos10010030

Zheng, J., Abulikemu, A., Wang, Y., Kong, M., & Liu, Y. (2022). Convection Initiation Associated with the Merger of an Immature Sea-Breeze Front and a Gust Front in Bohai Bay Region, North China: A Case Study. *Atmosphere*, *13*(5), 750. https://doi.org/10.3390/atmos13050750